Characterization of the Protein Components of *Nephila clavipes* Dragline Silk†

Alexander Sponner,‡,§ Bernhard Schlott,‡ Fritz Vollrath,§ Eberhard Unger,‡ Frank Grosse,‡ and Klaus Weisshart*,‡

Department of Biochemistry, Institute for Molecular Biotechnology, Beutenbergstrasse 11, 07745 Jena, Germany, and Department of Zoology, University of Oxford, South Parks Road, Oxford OX1 3PS, United Kingdom

Received November 2, 2004; Revised Manuscript Received December 20, 2004

ABSTRACT: Spider silk is predominantly composed of structural proteins called spider fibroins or spidroins. The major ampullate silk that forms the dragline and the cobweb's frame threads of *Nephila clavipes* is believed to be a composite of two spidroins, designated as Masp 1 and 2. Specific antibodies indeed revealed the presence of Masp 1 and 2 specific epitopes in the spinning dope and solubilized threads. In contrast, sequencing of specific peptides obtained from solubilized threads or gland urea extracts were exclusively homologous to segments of Masp 1, suggesting that this protein is more abundantly expressed in silk than Masp 2. The strength of immunoreactivities corroborated this finding. Polypeptides reactive against both Masp 1 and 2 specific antibodies were found to be expressed in the epithelia of the tail and different gland zones and accumulated in the gland secreted material. Both extracts of gland secretion and solubilized threads showed a ladder of polypeptides in the size range of 260−320 kDa in gel electrophoresis under reducing conditions, whereas gel filtration chromatography yielded molecular masses of the proteins of approximately 300−350 kDa. In the absence of a reducing agent, dimeric forms of the spidroins were observed with estimated molecular masses of 420−480 kDa according to gel electrophoresis and 550−650 kDa as determined by gel filtration chromatography. Depending on the preparation, some silk material readily underwent degradation, and polypeptides down to 20 kDa in size and less were detectable.

Spider silks display extraordinary mechanical properties (*1*, *2*). The major ampullate silk of orb-web spiders, for example, which is used by the spiders as the dragline (safety line), possesses high tensile strength combined with high viscoelasticity, yielding a toughness of the material that is superior to even high-tech synthetics (*3*). The major constituents of spider silk are fibrous proteins termed spidroins that are composed predominantly of the amino acids alanine and glycine (*4*). The precise amino acid composition of silk was found to be dependent on the spider's diet and environmental conditions and hence does vary within the same species (*5*−*10*).

The major ampullate spider silk of the orb-web spider *Nephila clavipes* is thought to be composed of at least two proteins that have been identified genetically. Two partial cDNAs, referred to as the major ampullate fibroin 1 (Masp 1) (*11*) and 2 (Masp 2) (*12*), respectively, have been reported.[1] cDNAs specific for Masp 1 and 2 have since become available for a variety of araneoid spiders, suggesting a common composite nature for different dragline silks in regard to their protein constituents (*11*−*15*). Masp 1 and 2 specific epitopes have been detected in the spinning dope and solubilized dragline silk and assigned in the former case to different polypetides (*16*, *17*).

It is assumed that alanine-rich regions of Masp 1 and 2 form crystallites that are responsible for the high tensile strength, whereas elasticity is contributed by glycine-rich stretches in both spidroins that locate predominantly to noncrystalline or amorphous areas (*18*). However, the contribution of the individual proteins to the mechanical properties of the dragline is still far from being fully understood. Since Masp 2 contains regularly spaced prolines that are detrimental to crystallite formation, it was reasoned that this type of spidroin is restricted to the amorphous noncrystalline part of dragline silk, whereas Masp 1 would reside predominantly in the crystalline areas (*19*).

According to a current model, the two spidroins are produced in different gland zones, referred to as the A and B zones (*20*−*22*). As deduced from the amino acid composition, tissue cells in the tail and the A zone are believed to secrete Masp 2, whereas in the B zone Masp 1 along with little Masp 2 is synthesized (*22*, *23*). The model predicts that Masp 2 will form the bulk of the fiber, with Masp 1 adding a coat layer. However, this view of the quantitative relationship between Masp 1 and Masp 2 is in conflict with several observations. First, in immunoblots, Masp 1 is the dominantly stained protein, albeit an effect of the antibodies' avidities cannot be ruled out (*16*); second, on the basis of RNA lengths and the abundance of cDNA clones, the ratio of Masp 1 to Masp 2 is estimated to be of the order of 3:2

† This work was supported by Bundesministerium für Forschung und Bildung (BMBF FKZ 0311130), Bundesministerium für Landwirtschaft (BML FKZ 98NR049), Thueringer Ministerium für Wissenschaft, Forschung und Kultur (TMWFK B307-99-001), US-AFOSR (F49620-03-1-0111), and European Commission (GSRD-CT-2002-00738).

* Corresponding author. Present address: Carl Zeiss Jena GmbH, Carl-Zeiss-Promenade 10, 07745 Jena, Germany. Phone: +49-3641-642268. Fax: +49-3641-643144. E-mail: weisshart@zeiss.de.

‡ Institute for Molecular Biotechnology.

§ University of Oxford.

[1] Abbreviations: SDS−PAGE, sodium dodecyl sulfate−polyacrylamide gel electrophoresis; IEF, isoelectric focusing; Masp, major ampullate spidroin; LiSCN, lithium rhodanide; LiBr, lithium bromide; Hfip, hexafluorisopropanol; PBS, phosphate-buffered saline.

10.1021/bi047671k CCC: $30.25
Published on Web 03/02/2005

(*12*); and third, no evidence for proline, the characteristic residue for Masp 2, was obtained by NMR spectroscopy on U-^{13}C-D-glucose-labeled silk (*24*).

In the work reported herein, we have reinvestigated the protein composition of the major ampullate silk. We provide unambiguous evidence for two distinct polypeptides and show their ubiquitous expression within the gland tissues. We further give evidence of a higher abundance of Masp 1 in the spinning dope and the thread and reveal immunological relationships of both Masps to spidroins synthesized in other glands.

MATERIALS AND METHODS

Cloning, Expression, and Purification of Repetitive Spidroin Sequences. Masp 1 and 2 positive cDNA clones (*17*) were used to amplify respective repetitive sequences. The primers used provided a distal *Eco*RI site and a proximal *Nde*I site to an ATG in-frame codon on the 5′-end and a *Bam*HI site after a STOP codon at the 3′-end. Primer pairs used were 5′-TTTGAATTCCATATGGCAGCAGCTGGTGGTGTTAGAC-3′/5′-TTTGGATCCTTAAGCAGACGCCCCAGAACCAAC-3′ for Masp 1 and 5′-TTTGAATTCCATATGCAACAAGGACCATCTGGACCA-3′/5′-TTTGGATCCTTACGCTGGTCCATATCCACCAGG-3′ as well as 5′-TTTGAATTCCATATGTCTGGTCCTGGAATCGCAGCT-3′/5′-TTTGGATCCTTAGGAAGCTTGAGAACCTGGCCC-3′ for Masp 2, respectively. Thus, in the case of Masp 1 nucleotides 1693−1935, corresponding to amino acids 565−645 (designated as S1R), and for Masp 2 nucleotides 1228−1416 (amino acids 410−472, S2R) as well as nucleotides 1429−1581 (amino acids 477−527, S2CR) of the published sequences were covered (*11*, *12*, *25*). Note that S1R and S2R sequences correspond to the highly repetitive parts of spidroins. S2CR represents a stretch in Masp 2 that links the highly repetitive sequences with the conserved C-terminus. It displays an intermediate repetitive character. The amplified sequences were cloned via *Eco*RI and *Bam*HI into pBlueskript KS II+ (Stratagene) to yield plasmids pBS/S1R, pBS/S2R, and pBS/S2CR, and the clones were confirmed by sequencing. For cloning into the bacterial pET expression vectors (*40*), the sequences were subcloned via the *Nde*I and *Bam*HI sites to obtain pET/S1R, pET/S2R, and pET/S2CR. The used expression vector pET15a provides an N-terminal histidine tag (his-tag). Expression of the fusion peptides termed H_6-S1R, H_6-S2R, and H_6-S2CR was done in the *E. coli* BL21(DE3) strain, and the peptides were purified on Talon resin (ClonTech) according to the supplier's instructions. Protein concentrations were determined with the BioRad Protein Assay Kit using IgG as a standard. Clones expressing the conserved C-termini (H_6-S1C, nucleotides 1933−2247, amino acids 645−748 for spidroin 1; H_6-S2C, nucleotides 1561−1884, amino acids 521−627 for spidroin 2) have been described in more detail elsewhere (*17*).

Antibodies. Polyclonal sera were generated in rabbits according to standard procedures by Biogenes (Berlin) (*26*). For the production of anti-sera against the silk threads, approximately 1 mg of reeled material containing major and minor ampullate filaments, which had been extensively washed in PBS (S-pbs) or treated with trypsin−EDTA solution (Gibco BRL) followed by washing with PBS (S-try), was used per injection. In both cases, a glycocomponent layer is to a great extent washed off (*27*). Silk was sheared in a Polytron prior to injection. For the production of anti-sera against the fusion peptides H_6-S1R, H_6-S2R, and H_6-S2CR, 400 μg of protein was used per injection. To remove reactivity against bacterial proteins in the latter cases, the sera were incubated with a nitrocellulose (NC) strip to which the antigen had been immobilized. Bound antibodies were eluted with an acidic buffer and neutralized (*26*). Sera against C-terminal conserved parts of spidroins 1 and 2 have been described previously (*17*). Cross-reactive antibodies were adsorbed to an NC strip to which the cross-reactive protein had been blotted. To this end, serum S1R was adsorbed to H_6-S2R, and serum S2R to H_6-S1R, to yield cross-reactive free anti-sera S1Rx and S2Rx. Likewise, S1C and S2C sera were cross-adsorbed against H_6-S2C and H_6-S1C proteins, respectively, to yield anti-sera S1Cx and S2Cx.

Spider Handling. Female *Nephila clavipes* spiders, collected in Florida (USA), were purchased from Mascarino Tarantulas (California, USA). The animals were kept in little cages with wooden frames at 80% humidity. Under these conditions, construction of webs is limited. Webs were sprayed with tap water every day. Twice a week, the spiders were fed *Musca domestica* flies or crickets ad libitum. For the experiments, spiders of the last three instar stages were used.

Preparation of Dragline Silk. Dragline threads were reeled from female *N. clavipes* spiders by a homemade device at ambient rates. The solid silk was dissolved in hexafluoroisopropanol (Hfip) (pH 4), saturated lithium rhodanide (LiSCN) (pH 9), or saturated lithium bromide (LiBr) (pH 8.5) to yield concentrations of about 10 mg/mL. Samples were centrifuged for 10 min at 10000*g*, and the supernatant was frozen in liquid nitrogen and stored at −70 °C until use. To test for stabilities, the silk material was incubated for prolonged times at room temperature and the sample checked for degradation by sodium dodecyl sulfate−polyacrylamide gel electrophoresis (SDS−PAGE) (*28*).

Preparation of Gland Extracts. Spiders were anaesthesized by carbon dioxide treatment. The spider's opisthosoma (abdomen) was separated from the cephalothorax and immediately dissected in spider Ringer (*29*) buffered with Tris base (100 mM) to pH 7.2. Liquid silk protein was isolated from freshly dissected glands by soaking them overnight in 8 M urea. Normally four glands were extracted in 100 μL of solution. Likewise, the jelly-like gel substance (gland secretion or spinning dope) was extracted after removal of the gland's epithelium. The clarified samples were stored at −70 °C until use. The stability of the silk material was analyzed by SDS−PAGE after incubation of the extracts for different times at room temperature.

For the preparation of different tissue zones, the gland was dissected in citrate buffer (*30*) and cut at the corresponding boundaries (*23*). The respective epithelium was then removed and immediately frozen in liquid nitrogen. To avoid degradation as much as possible, a protease inhibitor cocktail was added to the preparation and extraction buffers. End concentrations of the inhibitors were as follows: Bestatin, 40 μg/mL; E 64, 10 μg/mL; EDTA, 0.37 mg/mL; Pefablock, 0.2 mg/mL; Pepstatin, 0.7 μg/mL (all Roche); Aprotinin, 50 μg/mL (Sigma-Aldrich); and PMSF, 170 μg/mL (Roth). To the frozen material was added extraction buffer (6 M urea,

2 M thiourea, 0.5% CHAPS, 0.5% Triton X-100, 10 mM Tris-HCl pH 7.2) (40 μL for 10 gland tissue preparations). The tissue was disrupted by dounce homogenization in an Eppendorf tube with a fitting pestle and extracted overnight. Tail tissue and the gland secretion were treated likewise for comparison. The sample was centrifuged for 10 min at 10000*g* and the supernatant stored at −70 °C until use. To stimulate spidroin synthesis in the gland epithelia, the gland was partly depleted by silking the spider and waiting 1 h prior to dissection (*30*, *31*).

Gel Electrophoresis and Blotting of Solubilized Dragline Proteins. Silks dissolved in LiSCN, LiBr, or Hfip at 10 mg/mL were 10-fold diluted with 8 M urea or dialyzed against this solution if higher concentrations were needed. Ten-microgram portions of the samples were applied to precast 4−15% mini gradient or 5% discontinuous gels using the Mini-Protean II system (BioRad). For long runs to achieve a higher resolution for high-molecular-weight proteins, the Protean II xi Slab Cell (BioRad) was used, employing 20 cm glass plates.

Isoelectric focusing (IEF) was performed with the model 111 Mini IEF cell (BioRad) using preformed gels according to the supplier's instructions. The 2D SDS−PAGE IEF standards were used for calibration. Bio-Lyte 3/10 ampholytes were added to the samples (approximately 20 μg of protein) prior to focusing.

Gels were either Coomassie Brilliant Blue G250 stained or blotted to nitrocellulose (NC) filters. For blotting, gels were washed three times in fresh changes of transfer buffer (gel running buffer with 20% methanol added) for 5 min to remove, if necessary, the excess of urea and to equilibrate the gels for blotting. For dot blots, 1 μL of a saturated LiBr solution of silk threads (ca. 10 mg/ml), 1 μL of an 8 M urea extract of glands (four glands in 100 μL), or 1 μL fusion protein (approximately 2 mg/mL) was spotted onto NC filters. For denaturation of fusion proteins, a quarter volume of 4× Laemmli buffer (*28*) without bromphenol blue was added to the sample, followed by boiling for 2 min and rapidly cooling on ice. Filters were blocked in TBST (10 mM Tris-HCl pH 8, 150 mM NaCl, 0.05% Tween 20)/0.5% dry milk powder and incubated with silk specific antibodies. Dilutions were 1:1000 for S-pbs and S-try, 1:100 for non-cross-adsorbed sera (with the exception of S2CR), and 1:10 for cross-absorbed sera and S2CR. After being washed in TBST, the blots were incubated with the secondary antibody (dilution 1:1000) to which peroxidase was conjugated. After an additional wash step, the blots were developed by enhanced chemiluminescence (ECL) using a kit from Amersham Bioscience. Some blots were directly stained in 0.1% Coomassie or 0.5% Ponceau S solution (Sigma-Aldrich).

Size Exclusion Chromatography. Gland secretion extracted in urea and silk solubilized in Hfip were subjected to gel filtration chromatography on Sephadex G-200 using K26/70 columns (2.6 cm × 49.7 cm) (Amersham Bioscience). The total bed volume was approximately 175 mL. The void volume of the column was determined by the elution volume of Blue Dextran 200 and amounted to 81 mL. A 500 μL portion of the sample (ca. 5 mg of protein) was dialyzed against 6 M guanidinium hydrochloride in 0.1 M Tris-HCl pH 7.2. The reducing agent DTT was optionally added at a concentration of 10 mM to cleave disulfide bridges, and the sample was applied to the column. Using flow adaptors, the system was run on an FPLC system (Amersham Bioscience) at a flow rate of 0.25 mL/min. One hundred fractions of 2.5 mL each were collected. A 10 μL portion of each fraction was transferred to a well of a 96-well microtiter plate, and proteins were estimated with the BioRad Protein assay kit, monitoring the adsorbance at 595 nm in a spectrometer. In parallel, 50 μL of Strataclean beads (Stratagene) was added to one-fifth of each fraction. After 5 min of incubation with occasional shaking, beads were sedimented for 1 min at 10000*g* and suspended in Laemmli sample buffer (*28*). Bound proteins were analyzed by subjecting the beads to SDS−PAGE. The High Molecular Weight Gel Filtration Calibration Kit was used for calibrations in non-denaturing buffers. Standards included Thyroglobulin 669 kDa, Ferritin 440 kDa, Catalase 232 kDa, and Aldolase 158 kDa. Molecular weights were estimated by blotting the log values of the molecular weights against the K_{av} values. K_{av} values were calculated according to $K_{av} = (V_e - V_o)/(V_t - V_o)$, where V_e, V_o, and V_t represent the elution volume for the protein, the column void volume, and the total bed volume, respectively.

Sequencing of Spider Silk Peptides. Gland secretion was separated from tissue and extracted in a buffer containing 6 M urea, 2 M thiourea, 0.5% CHAPS, 0.5% Triton X-100, and 10 mM Tris-HCl pH 7.2. After separation by 5% SDS−PAGE, blotting on a PVDF membrane, and subsequent staining with Coomassie brilliant blue, individual bands were excised and microsequenced by Edman degradation using a Procise 494 HT protein sequencer (Applied Biosystems). Solubilized thread material, dialyzed against the same buffer, was treated likewise.

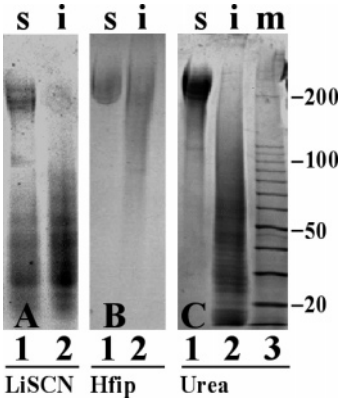

FIGURE 1: Solubilization and degradation of spider silk. Threads solubilized in LiSCN (panel A) and Hfip (panel B) as well as gland secretion extracted in urea (panel C) were analyzed shortly after preparation (s, lanes 1) or after extended incubation at room temperature (i, lanes 2). Incubation periods were as follows: panel A, 4 h; panel B, 168 h; panel C, 8 h. Samples were run on a 4−20% gradient gel, and proteins were visualized by Coomassie staining. Selected markers of a 10 kDa ladder (m, lane 3) are identified by their molecular weights.

RESULTS

Solubilization of Dragline Silk. Dragline silk threads were readily dissolved at concentrations of 10 mg/mL in LiSCN, LiBr, and Hfip. When the material was analyzed by gel electrophoresis, the Hfip sample displayed a ladder (or smear) of high-molecular-weight (hmw) polypeptides ranging in size between 260 and 320 kDa mass (Figure 1B, lane 1), as did the lithium bromide sample (data not shown). Only after

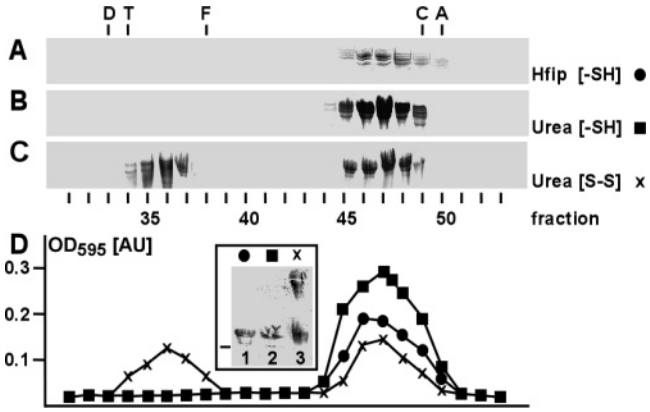

FIGURE 2: Size exclusion chromatography of gland secretion extracts and solubilized threads. Threads solubilized in Hfip (panel A) and urea gland secretion extracts (panels B and C) were fractionated in the presence (SH) or without (S-S) 10 mM DTT on gel filtration columns. Aliquots of the fractions were analyzed by SDS−PAGE and Coomassie staining (panels A−C). The elution profile (main peaks) of Blue Dextran 200, Thyroglobulin (669 kDa, T), Ferritin (440 kDa, F), Catalase (232 kDa, C), and Aldolase (158 kDa, A) are indicated above panel A. Aliquots of each fraction were also analyzed for the protein content, which is given in arbitrary units (AU) (panel D). The inset shows fractions of the starting material separated on a 5% denaturing gel under reducing (lanes 1 and 2) and nonreducing (lane 3) conditions. The bar indicates the position of the 250 kDa marker.

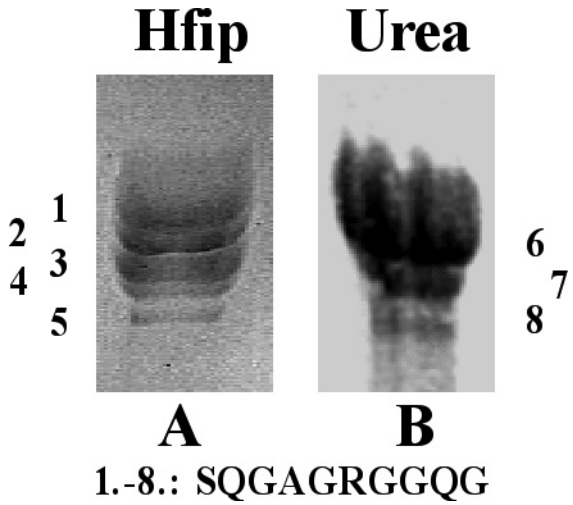

FIGURE 3: Amino acid sequence analysis. Amino acid sequences of polypeptides 1−8 obtained from solubilized thread (panel A) and gland secretion extracts (panel B) yielded the same dominant sequence, SQGAGRGGQG.

prolonged incubation for a week or longer at room temperature did some deterioration of the material become obvious in both cases (lane 2). In LiBr, the material started to degrade slightly faster. LiSCN solutions contained, besides the hmw polypeptides, proteins of lower molecular weight (lmw) (Figure 1A, lane 1). The hmw fraction was readily converted to the lmw fraction upon incubation at room temperature to polypeptides of 20 kDa mass and below. A nearly complete conversion was observed after approximately 4−8 h (lane 2). In general, for all solutes used, aged silk threads showed a slightly higher abundance of the lmw material than freshly spun silk (data not shown).

Solubilized silk was also obtained by extracting gland secretions (Figure 1C) or whole glands (data not shown) in 8 M urea. In either case, hmw polypeptides can be observed similar in size to the material obtained by solubilization of threads (lane 1). Especially with whole gland extracts and when the secretion was contaminated by epithelium, this hmw material was readily degraded upon incubation at room temperature (lane 2). Avoiding epithelium and adding protease inhibitors greatly stabilized the hmw material in secretion extracts.

Size Determination of Dragline Proteins. Size exclusion chromatography in denaturing aqueous buffers was performed to estimate the sizes of spidroins. If solubilized threads (Figure 2, panel A) or secretion extracts (panel B) treated with a reducing agent were applied to Sephadex G-200 columns, spidroins eluted in the major protein containing fractions that corresponded to a molecular mass distribution of 300−350 kDa compared to native marker proteins. If the reducing agent was omitted, a second peak became obvious in secretion extracts (panel C) that corresponded to a molecular size range of 550−650 kDa. The same outcome was obtained with solubilized threads (data not shown). The applied materials used for the gel filtration chromatographies were, in addition, analyzed by gel electrophoresis (inset of panel C). Under reducing conditions, the silk material migrates as a cluster of bands slightly slower than the 250 kDa marker, displaying a molecular mass distribution between 260 and 320 kDa (lanes 1 and 2). If the reducing agent was omitted, a second, higher molecular weight cluster of polypeptides of 420−480 kDa mass became evident (lane 3).

Sequence Analysis of Dragline Silk. We obtained sequence information on the high-molecular-weight material directly from excised bands. To this end, solubilized thread material (Figure 3A) and gland secretion extracts (Figure 3B) were subjected to gel electrophoresis. Long gel runs were employed to obtain as good a separation of single polypeptides as possible. After blotting, bands were visualized by Coomassie staining. Between three (panel B) and five bands (panel A) could be resolved and subjected to microsequencing. Despite a high background in some of the cycles, all bands yielded the same dominant sequence, SQGAGRGGQG, that is characteristic for Masp 1.

Characterization of Anti-sera. The peptide regions of Masp 1 and Masp 2 against which antibodies have been produced are depicted in Figure 4A. They include specificities against highly (S1R and S2R) and intermediate (S2CR) repetitive regions as well as conserved C-termini (S1C and S2C). In addition, anti-sera were obtained against PBS-washed (S-pbs) and trypsin-treated (S-try) threads. The sequences were expressed as his-tagged fusions termed H_6-S1C, H_6-S2C, H_6-S1R, H_6-S2R, and H_6-S2CR, respectively, allowing their purification by metal affinity chromatography (Figure 4B, panel a, lanes 2−6). H_6-S2CR was expressed about 10-fold less than the other fusion proteins (data not shown). The purified fusion proteins were approximately 10 kDa in size, which corresponds well with the calculated values. H_6-S2R was the only polypeptide showing additional higher molecular weight bands indicative of aggregation.

The S1C and S2C as well as the S1R and S2R anti-sera needed cross-adsorption (indicated by "x" after the name) in order to be specific for either of the respective fusion proteins (Figure 4B, compare panels b and c, d and e, f and g, h and i). The serum derived against H_6-S2CR showed only low titers (panel j). All efforts to obtain a higher titer failed

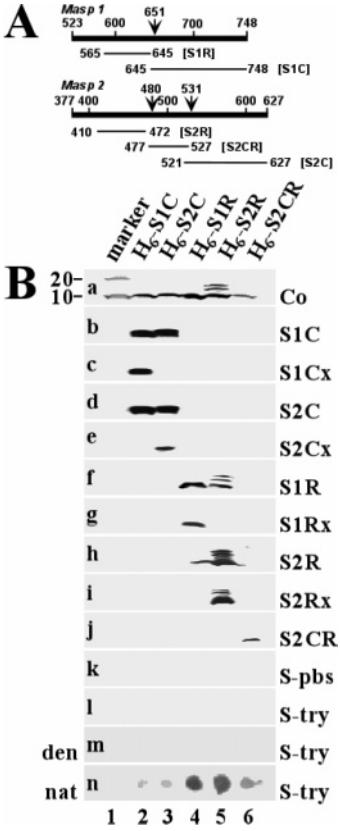

FIGURE 4: Reactivity of silk specific anti-sera. (A) Schematic drawing of the Masp 1 and 2 sequences. The numbers indicate amino acids. The arrows indicate the boundaries between highly repetitive, intermediate repetitive (only Masp 2), and conserved C-terminal sequences. The parts expressed as fusion peptides used to derive antibodies are indicated by thin bars. The names of the respective polypeptides are given in squared brackets. (B) Reaction of the indicated sera against purified fusion proteins in western blots (panels b−l) and dot blots (panels m−n). A Coomassie-stained gel of the fusion proteins is displayed in panel a, along with marker proteins with their molecular masses indicated in kDa. In panels m and n, the designated sera were reacted to denatured (den) and native (nat) fusion peptides, respectively. Detection of bound antibodies was by ECL.

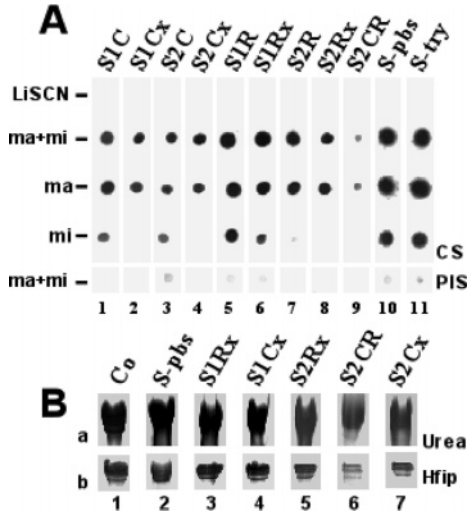

FIGURE 5: Specificity of silk specific anti-sera. (A) Dot blots of filaments solubilized in LiSCN. Solubilized major (ma) and minor (mi) ampullate filaments or a mixture of both (ma + mi) were spotted onto nitrocellulose filter strips. LiSCN served as a negative control. The filter strips were reacted with either converted sera (CS) or preimmune sera (PIS) as indicated. Detection was by ECL. (B) Western blots of gland secretion urea extracts (panel a) and threads solubilized in Hfip (panel b). The material was separated by SDS−PAGE. The gel was either Coomassie (Co) stained (lane 1) or blotted. The blots were incubated with the indicated antibodies (lanes 2−7). Bound antibodies were visualized by ECL.

in this case, suggesting that these special sequences are less immunogenic. S2CR did not show pronounced cross-reactivity against the other fusion proteins.

The sera obtained with silk threads either washed in PBS (S-pbs, panel k) or treated with trypsin (S-try, panel l) did not react with any of the denatured fusion proteins in western blots. To test if the silk sera were directed against structural and lacked sequence-specific epitopes of spidroins, fusion peptides were tested in their denatured state (panel m) or native form (panel n) in dot blots. Like in the western blots, the S-pbs and S-try sera did not react with the denatured proteins. In contrast, reactions were observed with the native proteins, demonstrating the presence of antibody titers against structural epitopes of spidroins. Titers were highest for the repetitive parts, intermediate for the less repetitive spidroin 2 region, and very low for the conserved C-termini.

Immunological Reactivity of Anti-sera against Dragline Silk. To determine if the anti-sera contained dragline silk specific antibodies, they were tested against silk filaments in dot blots. The filaments were dissolved in LiSCN, and the dissolved material was spotted on NC filters (Figure 5A). All the anti-sera were reactive, whereas the pre-immune sera did not show a specific staining. S-pbs and S-try sera reacted with both the major and minor ampullate filament material, as did the S1R, S1Rx, and non-cross-adsorbed S1C and S2C sera. S2CR, S2R, and cross-adsorbed S2Rx, S1Cx, and S2Cx sera, on the other hand, were specific for the major ampullate gland silk.

The anti-sera were further tested against the high-molecular-weight material of gland secretion extracts and solubilized threads (Figure 5B). All tested anti-sera were reactive against either material. The S-pbs, S-try (data not shown), and the Masp 1 specific sera yielded a stronger staining than sera obtained against Masp 2 peptides. In most cases, the starting material did not show pronounced bands but rather a smear, and it was not possible to discriminate polypetides on behalf of their antibody reactivity. A longer gel run was therefore performed, and we were able to distinguish up to four bands in urea extracts (Figure 6A) and up to eight bands in solubilized major ampullate filaments (Figure 6B). Whereas all bands of urea extracts were stained to different extents with the anti-sera S1Rx, band 3 was not reactive to the anti-serum S2Rx (compare lanes 2 and 3). Using solubilized filaments, four bands (1−4) were stained with both anti-sera, but to different extents. Two each of the bands were specific for either anti S1Rx (5 and 7) or anti S2Rx (6 and 8). Overall, the anti-sera S1Rx showed a stronger staining than anti-sera S2Rx if exposure times were kept within the linear range of the ECL reaction. Note that these antibodies showed similar titers against their respective fusion proteins (Figure 4B). We want to stress here that the resolution into different stained bands varied to a great extent between different preparations, and often it was not possible to assign any specificities in staining.

The existence of distinct anti-sera reactive silk material was corroborated by isoelectric focusing. Respective gels revealed two major fractions in urea extracts: two bands

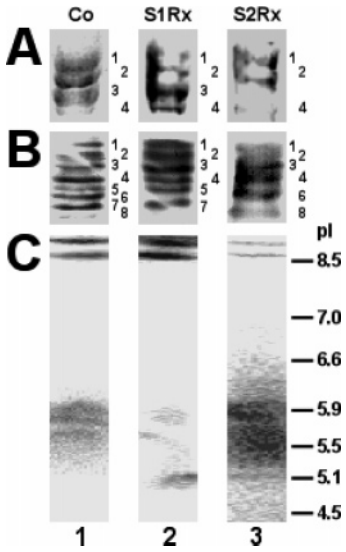

FIGURE 6: Detection of two different spidroin fractions. Gland secretion extracts (panel A) and solubilized threads (panel B) were subjected to SDS−PAGE (panel A). Gland secretion extracts were also applied to IF gels (panel C). The gels were either Coomassie (Co) stained (lane 1) or blotted to NC filters. Filters were reacted with either the S1Rx (lane 2) or the S2Rx (lane 3) anti-sera. Visualization of bound antibodies was performed by ECL. The visualized bands in panels A and B are numbered in the order of decreasing molecular weights. p*I* values of marker proteins are indicated at the right of panel C.

with p*I* 's above 8.5 and a diffuse stained area of polypeptides displaying p*I* 's between 5.1 and 5.9 (Figure 6C, lane 1). These p*I* 's correspond approximately to the calculated values for Masp 1 (p*I* 10.4) and Masp 2 (p*I* 6.3) based on the published sequences (*12*). The two fractions were differentially decorated by the anti-sera S1Rx and S2Rx. The polypeptides above a p*I* of 8.5 were stained strongly by the former and faintly by the latter (lane 2). On the other hand, the diffuse area around p*I* 5.5 reacted predominantly with S2Rx and showed little affinity for S1Rx (lane 3).The same outcome was obtained if solubilized major ampullate filaments were employed (data not shown).

Cross-Reactivities of Masp 1 and 2 Specific Sera to Spridroins of Other Gland Origin. The cross-adsorbed anti-sera specific for the repetitive parts were also tested with extracts from various other *N. clavipes*'*s* silk glands in western blots (Figure 7A). Each gland or secretion extract showed high-molecular-weight products (panel a). The S1Rx anti-sera reacted with, in addition to the major ampullate gland extracts, those derived from the minor ampullate gland (panel b, lanes 3 and 4). The S2Rx anti-sera showed cross-reactivities to the flagelliform and the piriform gland extracts (panel c, lanes 2, 4, and 5). Results obtained by western blotting were confirmed by dot blots in which urea extracts of the different glands had been spotted onto nitrocellulose strips (Figure 7B). Again, the minor and major ampullate silk reacted with the S1Rx serum (strip 1), whereas the piriform, flagelliform, and major ampullate silk were decorated by S2Rx (strip 2).

Expression of Major Ampullate Spidroins in Gland Tissues. The major ampullate (MA) gland shows a regionalized structure (*20*−*23*). It can be divided into the tail region, the ampulla, and the duct. The ampulla can be further subdivided into the A and B zones that are separated by an intermediate zone (Figure 8, panel D). Gland secretion (lane 1) and

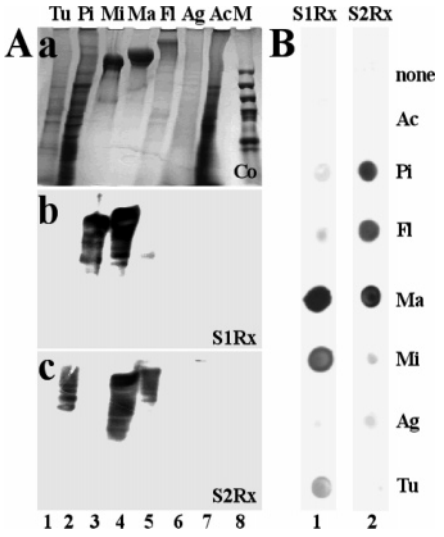

FIGURE 7: Cross-reactivity of spidroin 1 and 2 specific anti-sera to various gland extracts. Glands (lanes 1, 2, 5−7) or gland secretions (lanes 3 and 4) were extracted in urea and fractions either subjected to 4−15% SDS−PAGE (panel A) or spotted directly on NC filters (panel B). Gels were either Coomassie stained (a) or blotted to NC filters (b, c). Filters were reacted with the S1Rx (b and filter strip 1) and S2Rx anti-sera (c and filter strip 2). Bound antibodies were visualized by ECL. Abbreviations are as follows: AC, aciniform gland; AG, aggregate gland; FL, flagelliform or coronate gland; MA, major ampullate gland; MI, minor ampullate gland; PI, piriform gland; TU, tubuliform or cylindrical gland.

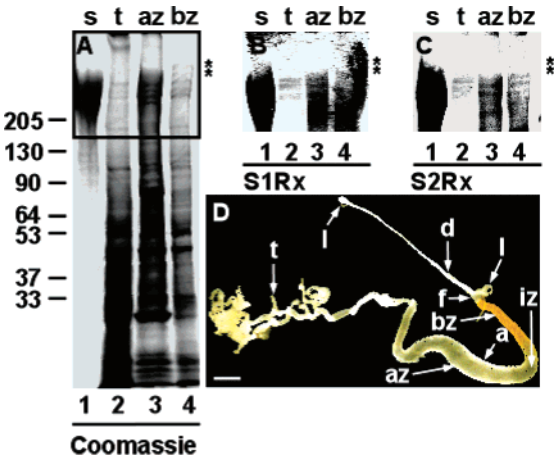

FIGURE 8: Expression of major ampullate spidroins in gland tissues. Gland secretion (lane 1) and tissue extracts from the tail (lane 2) as well as from the A (lane 3) and B (lane 4) zones were separated in triplicate. One gel was Coomassie stained (panel A). The positions of molecular weight markers run in parallel are identified by their molecular masses in kDa. The other two gels were blotted onto NC membranes and stained with anti-sera S1Rx (panel B) and S2Rx (panel C). Antibody detection was by ECL. The blots display only the part of the gel containing the high-molecular-weight material (frame in panel A). The asterisks indicate the positions of high-molecular-weight polypeptides found exclusively in the B zone. Panel D shows a stereomicroscope image of the major ampullate (MA) gland. The gland consists of a tubular tail (t), a sacklike ampulla (a), and a looped duct (d). Two loops (l) give rise to the three duct limbs. The duct ends in a spinneret (not shown in the image). The ampulla is divided into the A zone (az) and the B zone (bz), which are separated by an intermediate zone (iz). The end of the B zone is connected to the duct via a funnel (f). The bar equals 1 mm.

epithelia extracts of the tail (lane 2) and the A (lane 3) and B zones (lane 4) of unstimulated glands were prepared and analyzed by gel electrophoresis (panel A). In each case, high-

molecular-weight material was visible. Abundant low-molecular-weight material is also obvious in the tissue preparations. Some of the high-molecular-weight material was reactive to both anti-sera S1Rx (panel B) and S2Rx (panel C). The B zone displayed two high-molecular-weight polypeptides not seen in other extracts, indicated by asterisks, which were not reactive to either of the two anti-sera (compare lanes 4 of panels A−C). Using stimulated glands (glands 60 min after silking), the amounts of high-molecular-weight materials increased in the tissues, but again, S1Rx and S2Rx reactive material was found throughout all of them (data not shown).

DISCUSSION

In the present study we have characterized the major protein constituents of the dragline in respect to their abundance, their expressions within the gland, their stabilities, and the immunological relationships to other spidroins.

Degradation of Spider Silk Proteins. Degradation of solubilized silk was generally observed with any chaotropic solution used; however, the kinetics were quite different for specific solvents (Figure 1). Silk material degraded within hours in LiSCN but was quite stable in Hfip and LiBr for days and longer. We believe that degradation in chaotropic agents is induced chemically. The difference in stability could be caused by the different pH of the solutions facilitating hydrolytic degradation to different degrees. Whereas the LiSCN solution was strongly alkaline, with a pH around 9, the LiBr solution was slightly less alkaline, with a pH of around 8.5. On the other hand, the Hfip solution was acidic, with a pH of approximately 4. Aged threads displayed a slightly higher abundance of polypeptides in the lower size range (data not shown) in accordance with previous results (*32*). Hence, degradation processes might start within the solid thread. Environmental conditions, like oxidative processes and mechanical stress, could account for these observations.

Degradation was also observed in urea extracts of glands and gland secretion material (Figure 1C) in line with earlier observations (*30*, *33*). Since the decay of the material was less pronounced in gland secretion extracts without epithelium and high-molecular-weight proteins were stabilized in the presence of protease inhibitors, the synthesized and secreted silk is likely to be degraded by proteases present in the gland epithelium. Degradation starts N-terminally since the low-molecular-weight polypeptides react with the C-terminal specific antibodies (*17*). The presence of proteases in the gland epithelium suggests that proteolysis might work to remove misfolded, truncated, or otherwise unused spidroins. Since some spiders recycle their web material by digesting the silk, the proteolytic breakdown might serve the reusage of spun silk material.

Dragline Silk Consists of a Characteristic Ladder of High-Molecular-Weight Polypetides. By choosing appropriate conditions, materials can be obtained from both secretion extracts and solubilized threads that consist of a ladder of high-molecular-weight polypeptides with little contamination by smaller polypeptides. In ideal cases, three to five (Figure 3) and even up to eight polypeptides (Figure 4) can be resolved in SDS−PAGE. Under reducing conditions, polypeptides in the size range of 260−320 kDa can be found (Figure 2C, inset) which are likely to correspond to spidroin monomers. If the reducing agent is absent, a shift in the molecular mass to 420−480 kDa is observed. This species is probably related to disulfide-bridged dimers (*6*, *17*). The gain in molecular weight of the dimer compared to the monomer is less than 2-fold. However, calculations of high molecular weights are inaccurate in SDS−PAGE, and unusual running behaviors of spidroins as reported earlier might contribute to this discrepancy (*32*).

All the resolved bands contain polypeptides starting with the amino acid sequence SQGAGRGGQG specific for Masp 1 (Figure 3). Interestingly, Braunitzer and Wolff have determined the abundance of N-terminal residues in silk and found serine to be the predominant amino acid (*33*). The first three residues of this sequence (SQG), together with the two preceding amino acids LG, form the sequence motif LGXQG (X = G, S, N) that is believed to form type I β-turn structures at which the protein chain folds back on itself (*34*). Thus, these regions are exposed to the solvents and are easily accessible for proteolytic attack. All bands contain the true C-termini, as evidenced by specific anti-sera (Figure 5B), suggesting that the observed ladder is derived from N-terminal degradation by proteases and/or caused by glycosylation or other posttranslational modifications of the spidroins that might influence their molecular weights or running behavior (*27*, *35*, *36*). The extent of laddering and distribution in polypeptide sizes varied between different preparations. These heterogeneities might well depend on the physiological state of the spider (*5*−*10*). We want to point out that the observed ladder of peptides is present in preparations of unstimulated glands. We therefore disfavor the idea that our observed peptides correspond to those that are generated by translational pauses during de novo synthesis after gland stimulation (*31*).

Since nearly identical ladders of polypeptides of the same sizes can be found in the spinning dope and solubilized threads, the observed size heterogeneities in the latter seemed to be preformed in the gland-secrected material if one excludes the possibility of rapid limited degradation during the preparation. Whether the generation of a nested set of polypeptides is of biological relevance is not known. However, different size polypeptides could provide some flexibility to thread formation. Size constrictions imposed on the spidroin genes and proteins corroborate this assumption (A. Chinali, K.-H. Guehrs, and F. Grosse, unpublished results).

Earlier molecular mass estimations of the Masps have resulted in different outcomes: SDS−PAGE revealed values of 220 (*6*) and 320 kDa (*37*), whereas masses of up to 725 kDa were measured by gel filtration chromatography (*32*). On the basis of the largest reported mRNA sizes of 12 kb (*38*), the latter molecular mass seems to be too high for monomeric forms. Indeed, when Hfip-solubilized silk or gland secretion extracts were analyzed by gel filtration chromatography after treatment with a reducing agent, sizes of 300−350 kDa were calculated using standard proteins run under non-denaturing conditions (Figure 2). Since the silk samples were run in the chaotropic agent guanidinium chloride, the silk poylpetides are likely to be in an unfolded, elongated configuration and their sizes might be overestimated compared to the native standards. If samples were applied under nonreducing conditions, a second peak cor-

responding to 550−650 kDa became obvious that might correspond to the disulfide-linked dimers. The extent of that fraction varied quite pronouncedly from sample to sample (data not shown), and this putative dimeric form might correspond to the 725 kDa species of Jackson et al (*32*). It should be noted that, in the gel filtration chromatographies, the molecular weight of the dimeric form fell only slightly short to twice the value of the monomers.

Masp 1 and Masp 2 Contribute to Dragline Silk to Different Extents. The ratio of MaSp 1 and MaSp 2 was estimated to be about 3:2 in earlier studies (*12*). The extent of staining of gland and thread material with anti-sera specific for either of the spidroins would corroborate this finding (Figure 5B and Figure 6A,B). We cannot rule out avidity differences between the antibodies, but with the exception of S2CR anti-sera, the titers of all other unprurified anti-sera were nearly identical against the fusion peptides from which they were derived. Also, after cross-adsorption, the spidroin 1 specific anti-sera showed similar titers to their antigen as did the spidroin 2 specific anti-sera (Figure 4B).

By applying longer gel runs, we were able to assign Masp 1 and Masp 2 specific reactivities at least in part to different polypeptides (Figure 6A,B), as has been accomplished before (*16*). The prominent occurrence of doubly labeled bands might be due to several reasons: first, Masp 1 and Masp 2 polypeptides are of similar size and the limited gel resolution did not allow for their separation; second, degradation products of one species might comigrate as contaminants with the bands of the other species; and third, Masp 1 and 2 specific epitopes reside within the same polypeptide, as opposed to earlier suggestions (*16*, *39*). Our isoelectric focusing gels disfavor the last option (Figure 6C). Two fractions of different p*I* distributions were resolved that reacted to various extents with Masp 1 and 2 specifc anti-sera: the fraction of higher p*I* reacted predominantly with the S1Rx sera, and the fraction with the lower p*I* reacted against S2Rx, demonstrating two distinct populations of spidroins. It should be noted that the antibody staining pattern corresponded well with the calculated p*I* 's of Masp 1 (p*I* 10.4) and Masp 2 (p*I* 6.3). These data support the notion that Masp 1 and Masp 2 represent different polypeptides (*12*, *16*, *17*). The Masp 2 specific sera reacted in general to a lower extent to silk material, suggesting that this polypetide is expressed to a lesser extent.

We also have indirect evidence for two separate Masp 1 and 2 polypeptides based on genomic clones. Using DNA probes that were specific for those sequences that code for the characteristic repetitive protein sequences of Masp 1 and 2, respectively, no double-positive gDNA clone was found within a double representative genomic library (K. Weisshart, unpublished results). It seems, therefore, very unlikely that the unkown N-terminal sequences of Masp 1 contain typical repeat units that are believed to be characteristic for Masp 2 and vice versa and that the cross-adsorbed antibodies are not specific for either protein.

A high abundance of Masp 2 in the silk is challenged not only by the antibody reactivities but also by our sequencing results obtained with excised blotted polypeptides (Figure 3). The only clear sequence obtainable was the same for all polypeptides and was Masp 1 specific. It should be kept in mind that the obtained sequence might be prominent since it lies in a type I β-turn region and would therefore be highly accessible for proteolytic cleavage. Hence, other less prominent peptide sequences might be missing, given the high background we have experienced. On the other hand, chymotryptic peptide sequencing also revealed the exclusive presence of Masp 1 specific sequences (K.-H. Guehrs and F. Grosse, unpublished results). The presence of Masp 2 specific sequences has been proven by others before (*12*); however, such peptides were also severely underrepresented in those studies. In accordance with a low abundance of Masp 2 are, in addition, NMR studies of the major ampullate gland that failed to detect prolines which are specific for this spidroin (*34*). Taken together, the sequencing and the immunological data suggest the presence of at least two spidroins in the gland secretion (spinning dope) and the threads and attribute a higher abundance to Masp 1.

Immunological Relationships of Masps to Other Spidroins. Our anti-sera (S1Rx and S2Rx) specific for either of the two spidroins reacted not only with the content of the major ampullate gland but also in a characteristic way with extracts of other glands (Figure 7). The cross-reactions of S1Rx and S2Rx with extracts of the minor and flagelliform ampullate glands, respectively, can be explained by common sequence motifs present in the respective spidroins: MaSp 1 and MiSps both contain variations of the GXG motif, and MaSp 2 shares the GPGXX motif with Flags (*38*). Such cross-specific reactions have also been described by Fahnestock et al., who used spidroin specific sera generated with peptides representing the typical repeat units of the spidroins (*16*). The weak interaction of the MaSp 2 specific anti-sera against the extracts of the aciniform gland, as observed by Fahnestock et al., was not found with our MaSp 2 specific anti-sera, which might be due to the different sequences used for immunization. Indeed, there are only weak and very limited sequence homologies in the form of poly S and GPX (X, variable amino acid) sequences between the two spidroins (*12*, *40*). Instead we found a reaction of our Masp 2 specific serum with the content of the piriform gland, which had not been under scrutiny by Fahnestock and co-workers. The existence of a GPGXX motif in the piriform gland spidroins seems not to be inept, since this motif is suspected to confer elasticity to the silk (*38*, *41*). Such a property seems to be useful for the function of attachment disks, the silk of which is produced in the piriform glands (*42*). In a tangle of numerous fine threads, each of them must be equipped with a certain amount of elasticity to cooperatively resist the load imposed on them by the dragline thread that is used as a safety line and is attached to the disk. Unfortunately, no information is available at the moment about mechanical properties of piriform silk or about their sequences to support this view.

Masp 1 and 2 Specific Sequences Are Ubiquitously Expressed in Major Ampullate Gland Tissues. The formation of the spinning dope within the gland is thought to occur in separate steps (*23*). Amino acid compositions and structural data have led to the assumption that Masp 2 is synthesized in the A zone and forms the bulk spidroin, whereas Masp 1 is added as a coat layer in the B zone. Our data indicating Masp 1 as the more abundant spidroin are not in line with these assumptions. Moreover, we find ubiquitous synthesis of both Masp 1 and 2 throughout the gland tissues of the tail area as well as the A and B zones, demonstrating a common expression and secretion of both proteins (Figure

8). They also accumulate together in the spinning dope throughout the gland lumen (data not shown). Interestingly, the B zone tissue contained two high-molecular-weight polypeptides, not found in the tail and A zone, which were not reactive to antibodies specific for the repetitive regions of both Masp 1 and 2. It seems an attractive possibility that these and maybe other polypeptides provide the coat for the silk threads rather than Masp 1. Preliminary experiments indicate that the coat is in fact, immunologically distinct from the core (A. Sponner and K. Weisshart, unpublished results).

CONCLUSIONS

In this report we underscore the composite nature of the spider dragline silk with respect to its protein constituents. At least two spidroins contribute to the formation of the thread, with Masp 1 seemingly representing the predominant protein. Other spidroin-like proteins are likely to be added as a coat layer. The biochemical approach taken in this study should help in their identification and isolation.

ACKNOWLEDGMENT

The authors thank Ursula Stephan for excellent technical assistance.

REFERENCES

1. Gosline, J. M., Guerette, P. A., Ortlepp, C. S., and Savage, K. N. (1999) The mechanical design of spider silks: From fibroin sequence to mechanical function. *J. Exp. Biol. 202*, 3295−3303.
2. Cunniff, P. M., Fossey, S. A., Auerbach, M. A., Song, J. W., Kaplan, D., Adams, W. W., Eby, R. K., Mahoney, D. V., and Vezie, D. L. (1994) Mechanical and thermal properties of dragline silk from the spider Nephila clavipes. *Polym. Adv. Technol. 5*, 401−410.
3. Denny, M. W. (1980) Silks—their properties and functions, in The Mechanical Properties of Biological Meterials (Vincent, J. F. V., and Currey, J. D., eds.) *Symp. Soc. Exp. Biol. 34*, 247−272.
4. Kaplan, D., Fossey, S. A., Mello, C. M., Arcidiacono, S., Senecal, K., Muller, W., Stockwell, S., Beckwitt, R., Viney, C., and Kerkham, K. (1992) Biosynthesis and processing of silk proteins. *Mater. Res. Soc. Bull. 10*, 41−47.
5. Lombardi, S. J., and Kaplan, D. (1990) The amino acid composition of major ampullate gland silk (dragline) of Nephila clavipes (Araneae, Tetragnathidae). *J. Arachnol. 18*, 297−306.
6. Mello, C., Senecal, K., Yeung, B., Vourus, P., and Kaplan, D. (1994) in *In Silk Polymers: Material Science and Biotechnology* (Kaplan, D., Farmer, W. A., and Viney, C., eds.) pp 67−79, American Chemical Society, Washington, DC.
7. Vollrath, F., and Knight, D. P. (2001) Liquid crystalline spinning of spider silk. *Nature 410*, 541−548.
8. Prashad, B., Saund, A. K., and Mathur, N. K. (1972) Amino acid composition of spider silk. *Indian J. Biochem. Biophys. 9*, 351−352.
9. Casem, M. L., Turner, D., and Houchin, K. (1999) Protein and amino acid composition of silks from the cob weaver, Latrodectus hesperus (black widow). *Int. J. Biol. Macromol. 24*, 103−108.
10. Craig, C. L., Riekel, C., Herberstein, M. E., Weber, R. S., Kaplan, D., and Pierce, N. E. (2000) Evidence for diet effects on the composition of silk proteins produced by spiders. *Mol. Biol. Evol. 17*, 1904−1913.
11. Xu, M., and Lewis, R. V. (1990) Structure of a protein superfiber: spider dragline silk. *Proc. Natl. Acad. Sci. U.S.A. 87*, 7120−7124.
12. Hinman, M. B., and Lewis, R. V. (1992) Isolation of a clone encoding a second dragline silk fibroin. Nephila clavipes dragline silk is a two-protein fiber. *J. Biol. Chem. 267*, 19320−19324.
13. Guerette, P. A., Ginzinger, D. G., Weber, B. H., and Gosline, J. M. (1996) Silk properties determined by gland-specific expression of a spider fibroin gene family. *Science 272*, 112−115.
14. Gatesy, J., Hayashi, C., Motriuk, D., Woods, J., and Lewis, R. (2001) Extreme diversity, conservation, and convergence of spider silk fibroin sequences. *Science 291*, 2603−2605.
15. Lawrence, B. A., Vierra, C. A., and Moore, A. M. (2004) Molecular and Mechanical Properties of Major Ampullate Silk of the Black Widow Spider, Latrodectus hesperus. *Biomacromolecules 5*, 689−695.
16. Fahnestock, S. R., Yao, Z., and Bedzyk, L. A. (2000) Microbial production of spider silk proteins. *J. Biotechnol. 74*, 105−119.
17. Sponner, A., Unger, E., Grosse, F., and Weisshart, K. (2004) Conserved C-termini of spidroins are secreted by the major ampullate glands and retained in the silk thread. *Biomacromolecules 5*, 840−845.
18. Simmons, A. H., Michal, C. A., and Jelinski, L. W. (1996) Molecular orientation and two-component nature of the crystalline fraction of spider dragline silk. *Science 271*, 84−87.
19. Thiel, B. L., Guess, K. B., and Viney, C. (1997) Non-periodic lattice crystals in the hierarchical microstructure of spider (major ampullate) silk. *Biopolymers 41*, 703−719.
20. Kovoor, J. (1977) La soie et les glandes sericigenes des arachnides. *Annee Biol. 16*, 97−171.
21. Kovoor, J. (1990) The silk-gland system in some Tetragnathinae (Araneae: Araneidae). Comparative anatomy and histochemistry. *Acta Zool. Fenn. 190*, 215−222.
22. Vollrath, F., and Knight, D. P. (1999) Structure and function of the silk production pathway in the spider Nephila edulis. *Int. J. Biol. Macromol. 24*, 243−249.
23. Dicko, C., Vollrath, F., and Kenney, J. M. (2004) Spider Silk Protein Refolding Is Controlled by Changing pH. *Biomacromolecules 5*, 704−710.
24. Hijirida, D. H., Do, K. G., Michal, C., Wong, S., Zax, D., and Jelinski, L. W. (1996) ^{13}C NMR of Nephila clavipes major ampullate silk gland. *Biophys. J. 71*, 3442−3447.
25. Beckwitt, R., and Arcidiacono, S. (1994) Sequence conservation in the C-terminal region of spider silk proteins (Spidroin) from *Nephila clavipes* (Tetragnathidae) and *Araneus bicentenarius* (Araneidae). *J. Biol. Chem. 269*, 6661−6663.
26. Harlow, E., and Lane, D. P. (1988) *Antibodies: a laboratory manual*, Cold Spring Harbor Laboratory, Cold Spring Harbor, NY.
27. Augsten, K., Muehlig, P., and Hermann, C. (2000) Glycoproteins and skin-core structure in Nephila clavipes Spider silk observed by light and electron microscopy. *Scanning 22*, 12−15.
28. Laemmli, U. K. (1970) Cleavage of structural proteins during the assembly of the head of bacteriophage T4. *Nature 227*, 680−685.
29. Schartau, W., and Leidescher, T. J. (1983) Composition of the hemolymph of the tarantula Eurypelma-Californicum. *J. Comput. Physiol. 152*, 73−77.
30. Candelas, G., and Cintrón, I. (1981) A Spider Fibroin and its Synthesis. *J. Exp. Zool. 216*, 1−6.
31. Candelas, G., Candelas, T., Ortiz, A., and Rodriguez, O. (1983) Translational pauses during a spider fibroin synthesis. *Biochem. Biophys. Res. Commun. 116*, 1033−1038.
32. Jackson, C., and O'Brien, J. P. (1995) Molecular weight distribution of Nephila clavipes dragline silk. *Macromolecules 28*, 5975−5977.
33. Braunitzer, G., and Wolff, D. (1955) Vergleichende chemische Untersuchungen über die Fibroine von Bombyx mori und Nephila madagascariensis. *Z. Naturforsch. 10b*, 404−408.
34. Michal, C. A., and Jelinski, L. W. (1998) Rotational-echo double-resonance in complex biopolymers: a study of Nephila clavipes dragline silk. *J. Biomol. NMR 12*, 231−241.
35. Michal, C. A., Simmons, A. H., Chew, B. G., Zax, D. B., and Jelinski, L. W. (1996) Presence of phosphorus in Nephila clavipes dragline silk. *70*, 489−493.
36. Thiel, B. L., Kunkel, D. D., and Viney, C. (1994) Physical and Chemical Microstructure of Spider Dragline: A Study by Analytical Transmission Electron Microscopy. *Biopolymers 34*, 1089−1097.
37. Candelas, G. C., Ortiz, A., and Ortiz, N. (1989) Features of the cell-free translation of a spider fibroin mRNA. *Biochem. Cell. Biol. 67*, 173−176.
38. Hayashi, C. Y., Shipley, N. H., and Lewis, R. V. (1999) Hypotheses that correlate the sequence, structure, and mechanical properties of spider silk proteins. *Int. J. Biol. Macromol. 24*, 271−275.

39. Hinman, M. B., Jones, J. A., and Lewis, R. V. (2000) Synthetic spider silk: a modular fiber. *Trends Biotechnol. 18*, 374−379.
40. Hayashi, C. Y., Blackledge, T. A., and Lewis, R. V. (2004) Molecular and mechanical characterization of aciniform silk: uniformity of iterated sequence modules in a novel member of the spider silk fibroin gene family. *Mol. Biol. Evol. 21*, 1950−1959.
41. Hayashi, C. Y., and Lewis, R. V. (1998) Evidence from flagelliform silk cDNA for the structural basis of elasticity and modular nature of spider silks. *J. Mol. Biol. 275*, 773−784.
42. Lewis, R. V. (1992) Spider silk: The unraveling of a mystery. *Acc. Chem. Res. 25*, 392−398.

BI047671K